LETTER

https://doi.org/10.1038/s41586-019-1128-0

Climatic controls of decomposition drive the global biogeography of forest-tree symbioses

B. S. Steidinger[1,15], T. W. Crowther[2,15]*, J. Liang[3,4,15]*, M. E. Van Nuland[1], G. D. A. Werner[5], P. B. Reich[6,7], G. Nabuurs[8], S. de-Miguel[9,10], M. Zhou[3], N. Picard[11], B. Herault[12,13], X. Zhao[4], C. Zhang[4], D. Routh[2], GFBI consortium[14] & K. G. Peay[1]*

The identity of the dominant root-associated microbial symbionts in a forest determines the ability of trees to access limiting nutrients from atmospheric or soil pools[1,2], sequester carbon[3,4] and withstand the effects of climate change[5,6]. Characterizing the global distribution of these symbioses and identifying the factors that control this distribution are thus integral to understanding the present and future functioning of forest ecosystems. Here we generate a spatially explicit global map of the symbiotic status of forests, using a database of over 1.1 million forest inventory plots that collectively contain over 28,000 tree species. Our analyses indicate that climate variables—in particular, climatically controlled variation in the rate of decomposition—are the primary drivers of the global distribution of major symbioses. We estimate that ectomycorrhizal trees, which represent only 2% of all plant species[7], constitute approximately 60% of tree stems on Earth. Ectomycorrhizal symbiosis dominates forests in which seasonally cold and dry climates inhibit decomposition, and is the predominant form of symbiosis at high latitudes and elevation. By contrast, arbuscular mycorrhizal trees dominate in aseasonal, warm tropical forests, and occur with ectomycorrhizal trees in temperate biomes in which seasonally warm-and-wet climates enhance decomposition. Continental transitions between forests dominated by ectomycorrhizal or arbuscular mycorrhizal trees occur relatively abruptly along climate-driven decomposition gradients; these transitions are probably caused by positive feedback effects between plants and microorganisms. Symbiotic nitrogen fixers—which are insensitive to climatic controls on decomposition (compared with mycorrhizal fungi)—are most abundant in arid biomes with alkaline soils and high maximum temperatures. The climatically driven global symbiosis gradient that we document provides a spatially explicit quantitative understanding of microbial symbioses at the global scale, and demonstrates the critical role of microbial mutualisms in shaping the distribution of plant species.

Microbial symbionts strongly influence the functioning of forest ecosystems. Root-associated microorganisms exploit inorganic, organic[2] and/or atmospheric forms of nutrients that enable plant growth[1], determine how trees respond to increased concentrations[6] of CO_2, regulate the respiratory activity of soil microorganisms[3,8] and affect plant species diversity by altering the strength of conspecific negative density dependence[9]. Despite the growing recognition of the importance of root symbioses for forest functioning[1,6,10] and the potential to integrate symbiotic status into Earth system models that predict functional changes to the terrestrial biosphere[10], we lack spatially explicit quantitative maps of root symbioses at the global scale. Quantitative maps of tree symbiotic states would link the biogeography of functional traits of belowground microbial symbionts with their 3.1 trillion host trees[11], which are spread across Earth's forests, woodlands and savannahs.

The dominant guilds of tree root symbionts—arbuscular mycorrhizal fungi, ectomycorrhizal fungi, ericoid mycorrhizal fungi and nitrogen-fixing bacteria (N-fixers)—are all based on the exchange of plant photosynthate for limiting macronutrients. Arbuscular mycorrhizal symbiosis evolved nearly 500 million years ago, and ectomycorrhizal, ericoid mycorrhizal and N-fixer plant taxa have evolved multiple times from an arbuscular-mycorrhizal basal state. Plants that are involved in arbuscular mycorrhizal symbiosis comprise nearly 80% of all terrestrial plant species; these plants principally rely on arbuscular mycorrhizal fungi for enhancing mineral phosphorus uptake[12]. In contrast to arbuscular mycorrhizal fungi, ectomycorrhizal fungi evolved from multiple lineages of saprotrophic ancestors and, as a result, some ectomycorrhizal fungi are capable of directly mobilizing organic sources of soil nutrients (particularly nitrogen)[2]. Associations with ectomycorrhizal fungi—but not arbuscular mycorrhizal fungi—have previously been shown to enable trees to accelerate photosynthesis in response to increased concentrations of atmospheric CO_2 when soil nitrogen is limiting[6], and to inhibit soil respiration by decomposer microorganisms[3,8]. Because increased plant photosynthesis and decreased soil respiration both reduce atmospheric CO_2 concentrations, the ectomycorrhizal symbiosis is associated with buffering the Earth's climate against anthropogenic change.

In contrast to mycorrhizal fungi, which extract nutrients from the soil, symbiotic N-fixers (Rhizobia and Actinobacteria) convert atmospheric N_2 to plant-usable forms. Symbiotic N-fixers are responsible for a large fraction of biological soil-nitrogen inputs, which can increase nitrogen availability in forests in which N-fixers are locally abundant[13]. Symbioses with either N-fixers or ectomycorrhizal fungi often demand more plant photosynthate than does arbuscular mycorrhizal symbiosis[12,14,15]. Because tree growth and reproduction are limited by access to inorganic, organic and atmospheric sources of nitrogen, the distribution of root symbioses is likely to reflect environmental conditions that maximize the cost:benefit ratio of symbiotic exchange as well as physiological constraints on the different symbionts.

One of the earliest efforts[16] to understand the functional biogeography of plant root symbioses categorically classified biomes by their perceived dominant mycorrhizal type, and hypothesized that seasonal climates favour hosts that associate with ectomycorrhizal fungi (owing to the ability of these hosts to compete directly for organic nitrogen). By contrast, it has more recently been proposed that sensitivity to low temperatures has prevented N-fixers from dominating outside of the tropics, despite the potential for nitrogen fixation to alleviate nitrogen limitation in boreal forests[15,17]. However, global-scale tests of

[1]Department of Biology, Stanford University, Stanford, CA, USA. [2]Department of Environmental Systems Science, ETH Zürich, Zürich, Switzerland. [3]Department of Forestry and Natural Resources, Purdue University, West Lafayette, IN, USA. [4]Research Center of Forest Management Engineering of State Forestry and Grassland Administration, Beijing Forestry University, Beijing, China. [5]Department of Zoology, University of Oxford, Oxford, UK. [6]Department of Forest Resources, University of Minnesota, St Paul, MN, USA. [7]Hawkesbury Institute for the Environment, Western Sydney University, Penrith, New South Wales, Australia. [8]Wageningen University and Research, Wageningen, The Netherlands. [9]Department of Crop and Forest Sciences - Agrotecnio Center (UdL-Agrotecnio), Universitat de Lleida, Lleida, Spain. [10]Forest Science and Technology Centre of Catalonia (CTFC), Solsona, Spain. [11]Food and Agriculture Organization of the United Nations, Rome, Italy. [12]Cirad, UPR Forêts et Sociétés, University of Montpellier, Montpellier, France. [13]Department of Forestry and Environment, National Polytechnic Institute (INP-HB), Yamoussoukro, Côte d'Ivoire. [14]A list of participants and their affiliations appears in the online version of the paper. [15]These authors contributed equally: B. S. Steidinger, T. W. Crowther, J. Liang. *e-mail: tom.crowther@usys.ethz.ch; albeca.liang@gmail.com; kpeay@stanford.edu

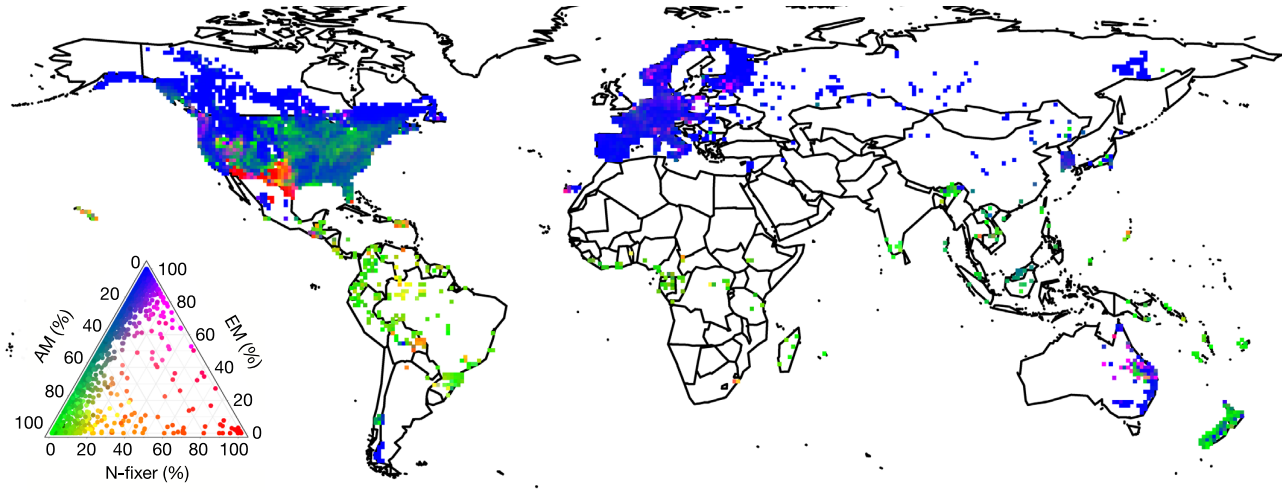

Fig. 1 | The global distribution of GFBi training data. The global map has $n = 2{,}768$ grid cells at a resolution of 1° × 1° latitude and longitude. Cells are coloured in the red, green and blue spectrum according to the percentage of total tree basal area occupied by N-fixer, arbuscular mycorrhizal (AM) and ectomycorrhizal (EM) tree symbiotic guilds, as indicated by the ternary plot.

these proposed biogeographical patterns and their climate drivers are lacking. To address this, we compiled a global ground-sourced survey database to reveal the numerical abundances of each type of symbiosis across the globe. Such a database is essential for identifying the potential mechanisms that underlie transitions in forest symbiotic state along climatic gradients[18,19].

We determined the abundance of tree symbioses using an extension of the plot-based Global Forest Biodiversity (GFB) database that we term the GFBi; this extended database contains over 1.1 million forest inventory plots of individual-based measurement records, from which we derive abundance information for entire tree communities (Fig. 1). Using published literature on the evolutionary histories of mycorrhizal and N-fixer symbioses, we assigned plant species from the GFBi to one of five root-associated symbiotic guilds: arbuscular mycorrhizal, ectomycorrhizal, ericoid mycorrhizal, N-fixer and weakly arbuscular or non-mycorrhizal. We then used the random-forest algorithm with *K*-fold cross-validation to determine the importance and influence of variables related to climate, soil chemistry, vegetation and topography on the relative abundance of each tree symbiotic guild (Fig. 2). Because decomposition is the dominant process by which soil nutrients become available to plants, we calculated annual and quarterly decomposition coefficients according to the Yasso07 model[20], which describes how temperature and precipitation gradients influence mass-loss rates of different chemical pools of leaf litter (with parameters fit using a previous global study of leaf decomposition) (Fig. 3, Supplementary Fig. 5). Finally, we projected our predictive models across the globe over the extent of global biomes that fell within the multivariate distribution of our model training data (Fig. 4, Supplementary Figs. 14, 15; see Methods for full description).

Our analysis shows that each one of the three most-numerically abundant guilds of tree symbiosis has a reliable environmental signature, with the four most-important predictors accounting for 81, 79 and 52% of the total variability in relative basal area for ectomycorrhizal, arbuscular mycorrhizal and N-fixer symbioses, respectively. Given the relative rarity of ericoid mycorrhizal and weakly arbuscular or non-mycorrhizal symbiotic states among trees, models for these symbioses lack strong predictive power—although the raw data do identify some local abundance hotspots for ericoid mycorrhizal symbiosis (Supplementary Fig. 1). As a result, we focus on the three major tree symbiotic states (ectomycorrhizal, arbuscular mycorrhizal and N-fixer). Despite the fact that data from North America and South America constitute 65% of the training data (at the 1°-by-1° grid scale), our models accurately predict the proportional abundances of the three major symbioses across all major geographical regions (Supplementary Fig. 10). The high performance of our models—which is robust to *K*-fold cross-validation and to rarefying samples such that all continents are represented with equal depth (Supplementary Figs. 11, 12)—suggests that regional variations in climate (including indirect effects on decomposition) and soil pH (for N-fixers) are the primary factors that influence the relative dominance of each guild at the global scale; geographical origin explained only approximately 2–5% of the variability in residual relative abundance (Supplementary Table 8, Supplementary Fig. 10).

Whereas a recent global analysis of root traits concluded that plant evolution has favoured a reduced dependence on mycorrhizal fungi[21], we find that trees that associate with the relatively more carbon-demanding and recently derived ectomycorrhizal fungi[12,14] represent the dominant tree symbiosis. By taking the average proportion of ectomycorrhizal trees, weighted by spatially explicit global predictions for tree stem density[11], we estimate that approximately 60% of tree stems on earth are ectomycorrhizal—despite the fact that only 2% of overall plant species associate with ectomycorrhizal fungi (versus nearly 80% that associate with arbuscular mycorrhizal fungi)[7]. Outside of the tropics, the estimate for the relative abundance of ectomycorrhizal symbiosis increases to approximately 80% of trees.

Turnover among the major symbiotic guilds results in a tri-modal latitudinal abundance gradient, in which the proportion of ectomycorrhizal trees increases (and the proportion of arbuscular mycorrhizal trees decreases) with distance from the equator and the upper quantiles of nitrogen-fixing trees reach a peak in abundance in the arid zone at around 30° N or S (Figs. 3a and 4). These trends are driven by abrupt transitional regions along continental climatic gradients (Fig. 2), which skew the distribution of symbioses among biomes (Fig. 3a) and drive strong patterns across geographical and topographic features that influence climate. Moving north or south from the equator, the first transitional zone separates warm (aseasonal) tropical broadleaf forests dominated by arbuscular mycorrhizal symbiosis (>75% median basal area versus 8% for ectomycorrhizal trees) from the rest of the world forest system, which is dominated by ectomycorrhizal symbiosis (Figs. 2a, b and 3a). The transition zone occurs across the globe at around 25° N and S, just beyond the dry tropical broadleaf forests (which have 25% of their basal area consisting of ectomycorrhizal trees) (Fig. 3a) in which average monthly temperature variation reaches 3–5 °C (temperature seasonality) (Fig. 2a, b).

Moving further north or south, the second transitional climate zone separates regions in which decomposition coefficients during the warmest quarter of the year are less than two (Fig. 3b gives the associated temperature and precipitation ranges). In North America and China, this transition zone occurs around 50° N, and separates the mixed arbuscular mycorrhizal and ectomycorrhizal temperate forests

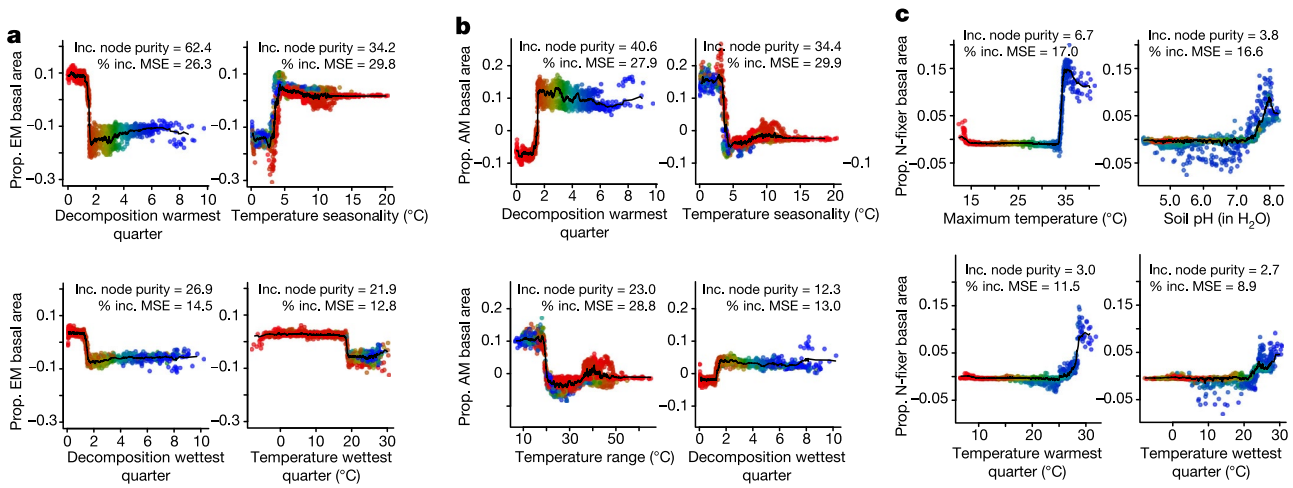

Fig. 2 | A small number of environmental variables predict the majority of global turnover in forest symbiotic status. a–c, Partial feature contributions of different environmental variables to forest symbiotic state. Each row plots the shape of the contribution of the four most-important predictors of the proportion of tree basal area that belongs to the ectomycorrhizal (**a**), arbuscular mycorrhizal (**b**) and N-fixer (**c**) symbiotic guilds ($n = 2{,}768$). Variables are listed in declining importance from left to right, as determined by the increase in node purity (inc. node purity), and with points coloured with a red to green to blue gradient according to their position on the x axis of the most-important variable (left-most panels for each guild), allowing cross-visualization between predictors. Each panel lists two measures of variable importance; inc. node purity (used for sorting) and percentage increase in mean square error (% inc. MSE) (see Supplementary Information). The abundance of each type of symbiont transitions sharply along climatic gradients, which suggests that sites near the threshold are particularly vulnerable to switching their dominant symbiont guild as climate changes. Warmest and wettest quarter, the warmest and wettest quarters of the year, respectively.

from their neighbouring ectomycorrhizal-dominated boreal forests (75 and 100% of their basal area, respectively, consisting of ectomycorrhizal trees) (Fig. 3a). This transitional decomposition zone is not present in western Europe, which has a temperature seasonality of >5 °C but lacks sufficiently wet summers to accelerate decomposition coefficients beyond the values that are associated with mixed arbuscular mycorrhizal and ectomycorrhizal forests. The latitudinal transitions in symbiotic state observed among biomes are mirrored by within-biome transitions along elevation gradients. For example, in tropical Mexico decomposition coefficients of less than two during the warmest and wetter quarters of the year occur along the slopes of the Sierra Madre, where a mixture of arbuscular-mycorrhizal and N-fixer woodlands in arid climates transition to ectomycorrhizal-dominated tropical coniferous forests (75% basal area) (Figs. 3a and 4a–c, Supplementary Figs. 16–18). The Southern Hemisphere—which lacks the landmass to support extensive boreal forests—experiences a similar latitudinal transition in decomposition rates along the ecotone that separates its tropical and temperate biomes, at around 28° S.

The abrupt transitions that we detected between forest symbiotic states along environmental gradients suggest that positive feedback effects may exist between climatic and biological controls of decomposition[10,20]. In contrast to arbuscular mycorrhizal fungi, some

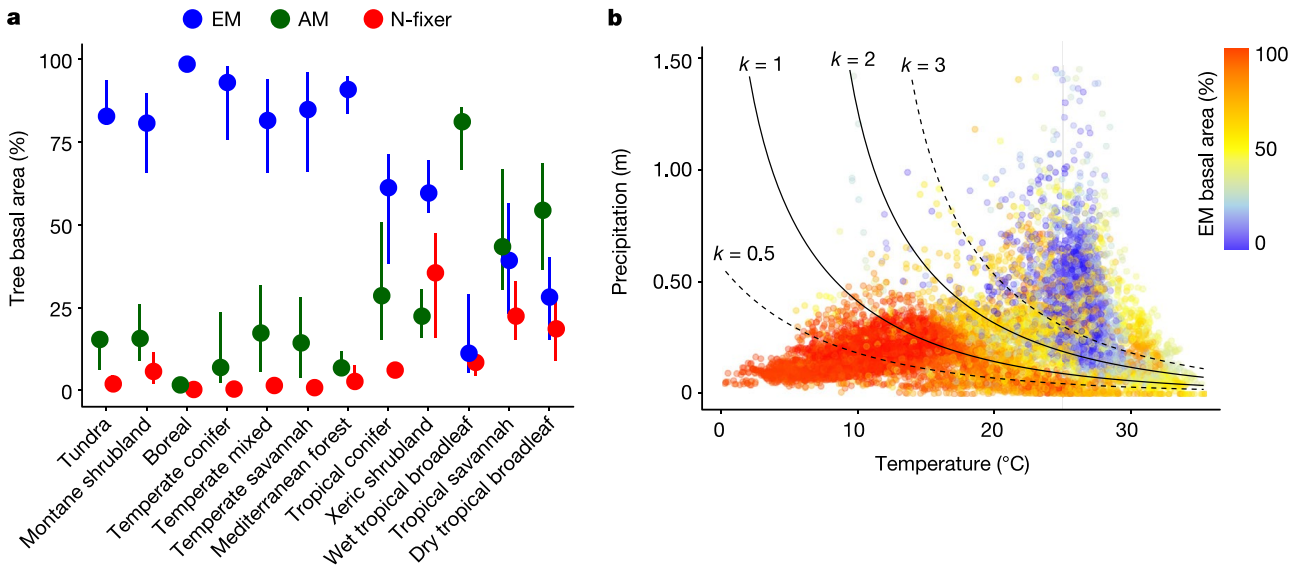

Fig. 3 | The distribution of forest symbiotic status across biomes is related to climatic controls over decomposition. a, Biome level summaries of the median ± 1 quartile of the predicted percentage of tree basal area per biome for ectomycorrhizal, arbuscular mycorrhizal and N-fixer symbiotic guilds ($n = 100$ random samples per biome). **b**, The dependency of decomposition coefficients (k, solid and dotted lines; in the region between the solid lines, the model transitions abruptly between dominant symbiotic status) on temperature and precipitation during the warmest quarter with respect to predicted dominance of mycorrhizal symbiosis. The transition from arbuscular mycorrhizal forests to ectomycorrhizal forests between $k = 1$ and $k = 2$ is abrupt, which is consistent with positive feedback between climatic and biological controls of decomposition.

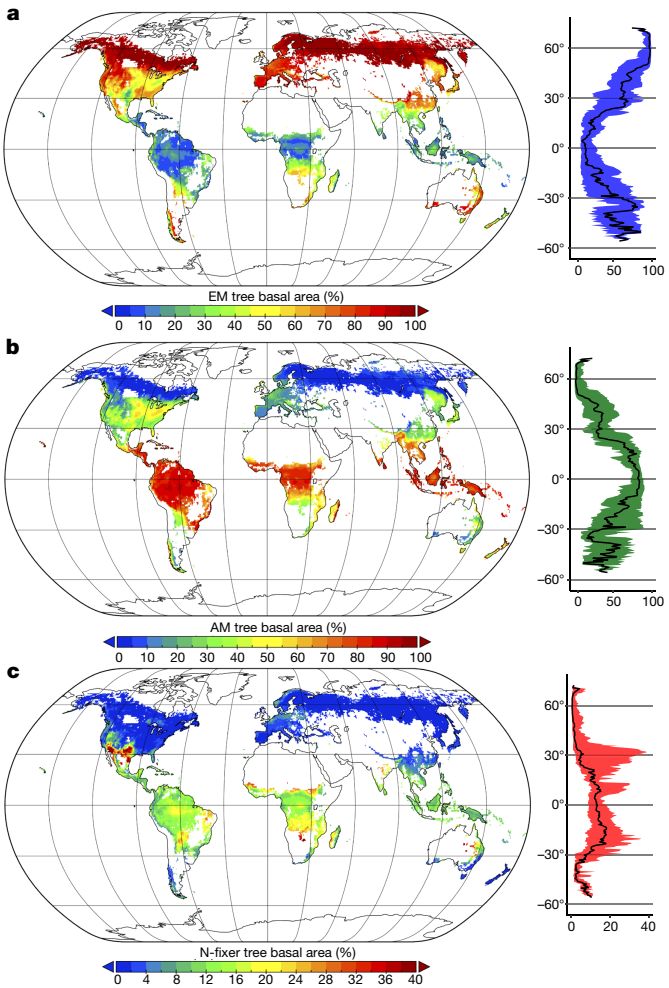

Fig. 4 | Global maps of predicted forest-tree symbiotic state. **a**–**c**, Maps (left) and latitudinal gradients (right; solid line indicates median; coloured ribbon spans the range between the 5% and 95% quantiles) of the percentage of tree basal area for ectomycorrhizal (**a**), arbuscular mycorrhizal (**b**) and N-fixer (**c**) symbiotic guilds. All projections are displayed on a 0.5°-by-0.5° latitude and longitude scale. $n = 28{,}454$ grid cells.

ectomycorrhizal fungi can use oxidative enzymes to mineralize organic nutrients from leaf litter and convert nutrients to plant-usable forms[2,5]. Relative to arbuscular mycorrhizal trees, the leaf litter of ectomycorrhizal trees is also chemically more resistant to decomposition, and has higher C:N ratios and higher concentrations of decomposition-inhibiting secondary compounds[10]. Thus, ectomycorrhizal leaf litter can exacerbate climatic barriers to decomposition and promote conditions in which ectomycorrhizal fungi have nutrient-acquiring abilities that are superior to those of arbuscular mycorrhizal fungi[5,10]. A recent game-theoretical model has shown that positive feedback effects between plants and soil nutrients can lead to local bistability in mycorrhizal symbiosis[22]. Such positive feedback effects are also known to cause abrupt ecosystem transitions along smooth environmental gradients between woodlands and grasses: trees suppress fires (which promotes seedling recruitment), whereas grass fuels fires that kill tree seedlings[23]. The existence of abrupt transitions also suggests that forests in transitional regions along decomposition gradients should be susceptible to marked turnover in symbiotic state with future environmental changes[23].

To illustrate the sensitivity of global patterns of tree symbiosis to climate change, we use the relationships that we observed for current climates to project potential changes in the symbiotic status of forests in the future. Relative to our global predictions that use the most-recent climate data, model predictions that use the projected climates for 2070 suggest that the abundance of ectomycorrhizal trees will decline by as much as 10% (using a relative concentration pathway of 8.5 W per m^2) (Supplementary Fig. 24). Our models predict that the largest declines in ectomycorrhizal abundance will occur along the boreal–temperate ecotone, where small increases in climatic decomposition coefficients cause abrupt transitions to arbuscular mycorrhizal forests (Fig. 2a, b). Although our model does not estimate the time lag between climate change and forest community responses, the predicted decline in ectomycorrhizal trees corroborates the results of common garden transfer and simulated warming experiments, which have demonstrated that some important ectomycorrhizal hosts will decline at the boreal–temperate ecotone under altered climate conditions[24].

The change in dominant nutrient-exchange symbioses along climate gradients highlights the interconnection between atmospheric and soil compartments of the biosphere. The transition from arbuscular mycorrhizal to ectomycorrhizal dominance corresponds with a shift from phosphorus to nitrogen limitation of plant growth with increasing latitude[25,26]. Including published global projections of total soil nitrogen or phosphorus, microbial nitrogen or soil phosphorus fractions (labile, occluded, organic and apatite) did not increase the amount of variation explained by the model, or alter the variables identified as most important; we therefore dropped these projections from our analysis. However, our finding that climatic controls of decomposition are the best predictors of dominant mycorrhizal associations provides a mechanistic link between symbiont physiology and climatic controls on the release of soil nutrients from leaf litter. These findings are consistent with Read's hypothesis[16] that slow decomposition at high latitudes favours ectomycorrhizal fungi owing to their increased capacity to liberate organic nutrients[2]. Thus, although more experiments are necessary to understand the specific mechanism by which nutrient competition favours the dominance of arbuscular mycorrhizal or ectomycorrhizal symbioses[18], we propose that the latitudinal and elevational transitions from arbuscular-mycorrhizal-dominated to ectomycorrhizal-dominated forests be named 'Read's rule'.

Our analyses focus on prediction at large spatial scales that are appropriate to the available data, but our findings with respect to Read's rule also provide insight into how soil factors structure the fine-scale distributions of tree symbioses within our grid cells. For example, at a coarse scale, we find that ectomycorrhizal trees are relatively rare in many wet tropical forests; however, individual tropical sites in our raw data span the full range from 0 to 100% basal area dominated by ectomycorrhizal trees. In much of the wet tropics, these ectomycorrhizal-dominated sites exist as outliers within a matrix of predominantly arbuscular mycorrhizal trees. In an apparent exception that proves Read's rule, in aseasonal, warm neotropical climates—which accelerate leaf decomposition and promote the regional dominance of arbuscular mycorrhizal symbiosis (Fig. 3)—ectomycorrhizal-dominated tree stands can develop in sites in which poor soils and recalcitrant litter slow the rates of decomposition and nitrogen mineralization[18,27]. Landscape-scale variation in the relative abundance of symbiotic states also changes along climate gradients: variability is highest in xeric and temperate biomes (Supplementary Figs. 3, 4), which suggests that the potential of local nutrient variability to favour particular symbioses is contingent on climate.

Whereas ectomycorrhizal trees are associated with ecosystems in which plant growth is thought to be primarily nitrogen-limited, N-fixer trees are not. Our results highlight the global extent of the apparent 'nitrogen cycling paradox' in which some metrics suggest that nitrogen limitation is greater in the temperate zone[25,26] and yet nitrogen-fixing trees are relatively more common in the tropics[15,28] (Fig. 3a). We find that N-fixers—which we estimate represent 7% of all trees—dominate forests with annual maximum temperatures >35 °C and alkaline soils, particularly in North America and Africa (Fig. 2c). N-fixers have the highest relative abundance in xeric shrublands (24%), tropical savannahs (21%) and dry broadleaf forest biomes (20%), but are nearly absent from boreal forests (<1%) (Figs. 3a and 4). The decline in N-fixer tree

abundance with increasing latitude that we observed is also associated with a previously documented latitudinal shift in the identity of nitrogen-fixing microorganisms, from facultative rhizobial N-fixers in tropical forests to obligate actinorhizal N-fixers in temperate forests[28]. Our data are not capable of fully disentangling the several hypotheses that have previously been proposed to reconcile the nitrogen cycling paradox[15]. However, our results are consistent with the model prediction[17] and regional empirical evidence[19,29,30] that nitrogen-fixing trees are particularly important in arid biomes. Based primarily on the observed positive nonlinear association of the relative abundance of N-fixers with the mean temperature of the hottest month (Fig. 2c), our models predict a twofold increase in relative abundance of N-fixers when transitioning from humid to dry tropical forest biomes (Fig. 3a).

Although soil microorganisms are a dominant component of forests in terms of both diversity and ecosystem functioning[5,6,10], identifying global-scale microbial biogeographical patterns remains an ongoing research priority. Our analyses confirm that Read's rule—which is one of the first proposed biogeographical rules specific to microbial symbioses—successfully describes global transitions between mycorrhizal guilds. More generally, climate driven turnover among the major symbioses between plants and microorganisms represents a fundamental biological pattern in the Earth system, as forests transition from low-latitude arbuscular mycorrhizal through N-fixer to high-latitude ectomycorrhizal ecosystems. The predictions of our model (available in the Supplementary Data as global raster layers) can now be used to represent these critical ecosystem variations in global biogeochemical models that are used to predict climate–biogeochemical feedback effects within and between trees, soils and the atmosphere. Additionally, the raster layer that contains the proportion of nitrogen-fixing trees can be used to map potential symbiotic nitrogen fixation, which links atmospheric pools of carbon and nitrogen. Future work can extend our findings to incorporate multiple plant growth forms and non-forested biomes (in which similar patterns are likely to exist) to generate a complete global perspective. Our predictive maps leverage a comprehensive global forest dataset to generate a quantitative global map of forest tree symbioses, and demonstrate how nutritional mutualisms are coupled with the global distribution of plant communities.

Online content

Any methods, additional references, Nature Research reporting summaries, source data, statements of data availability and associated accession codes are available at https://doi.org/10.1038/s41586-019-1128-0.

Received: 27 April 2018; Accepted: 21 March 2019;
Published online 15 May 2019.

1. Batterman, S. A. et al. Key role of symbiotic dinitrogen fixation in tropical forest secondary succession. *Nature* **502**, 224–227 (2013).
2. Shah, F. et al. Ectomycorrhizal fungi decompose soil organic matter using oxidative mechanisms adapted from saprotrophic ancestors. *New Phytol.* **209**, 1705–1719 (2016).
3. Averill, C., Turner, B. L. & Finzi, A. C. Mycorrhiza-mediated competition between plants and decomposers drives soil carbon storage. *Nature* **505**, 543–545 (2014).
4. Clemmensen, K. E. et al. Roots and associated fungi drive long-term carbon sequestration in boreal forest. *Science* **339**, 1615–1618 (2013).
5. Cheeke, T. E. et al. Dominant mycorrhizal association of trees alters carbon and nutrient cycling by selecting for microbial groups with distinct enzyme function. *New Phytol.* **214**, 432–442 (2017).
6. Terrer, C., Vicca, S., Hungate, B. A., Phillips, R. P. & Prentice, I. C. Mycorrhizal association as a primary control of the CO_2 fertilization effect. *Science* **353**, 72–74 (2016).
7. Brundrett, M. C. & Tedersoo, L. Evolutionary history of mycorrhizal symbioses and global host plant diversity. *New Phytol.* **220**, 1108–1115 (2018).
8. Averill, C. & Hawkes, C. V. Ectomycorrhizal fungi slow soil carbon cycling. *Ecol. Lett.* **19**, 937–947 (2016).
9. Bennett, J. A. et al. Plant–soil feedbacks and mycorrhizal type influence temperate forest population dynamics. *Science* **355**, 181–184 (2017).
10. Phillips, R. P., Brzostek, E. & Midgley, M. G. The mycorrhizal-associated nutrient economy: a new framework for predicting carbon-nutrient couplings in temperate forests. *New Phytol.* **199**, 41–51 (2013).
11. Crowther, T. W. et al. Mapping tree density at a global scale. *Nature* **525**, 201–205 (2015).
12. van der Heijden, M. G., Martin, F. M., Selosse, M. A. & Sanders, I. R. Mycorrhizal ecology and evolution: the past, the present, and the future. *New Phytol.* **205**, 1406–1423 (2015).
13. Binkley, D., Sollins, P., Bell, R., Sachs, D. & Myrold, D. Biogeochemistry of adjacent conifer and alder-conifer stands. *Ecology* **73**, 2022–2033 (1992).
14. Leake, J. et al. Networks of power and influence: the role of mycorrhizal mycelium in controlling plant communities and agroecosystem functioning. *Can. J. Bot.* **82**, 1016–1045 (2004).
15. Hedin, L. O., Brookshire, E. N. J., Menge, D. N. L. & Barron, A. R. The nitrogen paradox in tropical rainforest ecosystems. *Annu. Rev. Ecol. Evol. Syst.* **40**, 613–635 (2009).
16. Read, D. J. Mycorrhizas in ecosystems. *Experientia* **47**, 376–391 (1991).
17. Houlton, B. Z., Wang, Y.-P., Vitousek, P. M. & Field, C. B. A unifying framework for dinitrogen fixation in the terrestrial biosphere. *Nature* **454**, 327–330 (2008).
18. Peay, K. G. The mutualistic niche: mycorrhizal symbiosis and community dynamics. *Annu. Rev. Ecol. Evol. Syst.* **47**, 143–164 (2016).
19. Pellegrini, A. F. A., Staver, A. C., Hedin, L. O., Charles-Dominique, T. & Tourgee, A. Aridity, not fire, favors nitrogen-fixing plants across tropical savanna and forest biomes. *Ecology* **97**, 2177–2183 (2016).
20. Tuomi, M. et al. Leaf litter decomposition—estimates of global variability based on Yasso07 model. *Ecol. Modell.* **220**, 3362–3371 (2009).
21. Ma, Z. et al. Evolutionary history resolves global organization of root functional traits. *Nature* **555**, 94–97 (2018).
22. Lu, M. & Hedin, L. O. Global plant–symbiont organization and emergence of biogeochemical cycles resolved by evolution-based trait modelling. *Nat. Ecol. Evol.* **3**, 239–250 (2019).
23. Scheffer, M., Carpenter, S., Foley, J. A., Folke, C. & Walker, B. Catastrophic shifts in ecosystems. *Nature* **413**, 591–596 (2001).
24. Reich, P. B. et al. Geographic range predicts photosynthetic and growth response to warming in co-occurring tree species. *Nat. Clim. Change* **5**, 148 (2015).
25. McGroddy, M. E., Daufresne, T. & Hedin, L. O. Scaling of C:N:P stoichiometry in forests worldwide: implications of terrestrial redfield-type ratios. *Ecology* **85**, 2390–2401 (2004).
26. Reich, P. B. & Oleksyn, J. Global patterns of plant leaf N and P in relation to temperature and latitude. *Proc. Natl Acad. Sci. USA* **101**, 11001–11006 (2004).
27. Corrales, A., Mangan, S. A., Turner, B. L. & Dalling, J. W. An ectomycorrhizal nitrogen economy facilitates monodominance in a neotropical forest. *Ecol. Lett.* **19**, 383–392 (2016).
28. Menge, D. N., Lichstein, J. W. & Angeles-Pérez, G. Nitrogen fixation strategies can explain the latitudinal shift in nitrogen-fixing tree abundance. *Ecology* **95**, 2236–2245 (2014).
29. Liao, W., Menge, D. N. L., Lichstein, J. W. & Ángeles-Pérez, G. Global climate change will increase the abundance of symbiotic nitrogen-fixing trees in much of North America. *Glob. Change Biol.* **23**, 4777–4787 (2017).
30. Gei, M. et al. Legume abundance along successional and rainfall gradients in neotropical forests. *Nat. Ecol. Evol.* **2**, 1104–1111 (2018).

Acknowledgements This work was made possible by the Global Forest Biodiversity Database, which represents the work of over 200 independent investigators and their public and private funding agencies (see Supplementary Acknowledgements).

Reviewer information *Nature* thanks Martin Bidartondo, David Bohan and the other anonymous reviewer(s) for their contribution to the peer review of this work.

Author contributions K.G.P. and T.W.C. conceived the study; T.W.C., J.L., P.B.R., G.N., S.d.-M., M.Z., N.P., B.H., X.Z. and C.Z. conceived and organized the GFBi database; K.G.P., B.S.S., G.D.A.W. and M.E.V.N. compiled the symbiosis database; B.S.S. carried out the primary data analysis; M.E.V.N. and D.R. contributed to data compilation and analysis; B.S.S., T.W.C., M.E.V.N. and K.G.P. wrote the initial manuscript; B.S.S., T.W.C., J.L., M.E.V.N., G.D.A.W., P.B.R., G.N., S.d.-M., M.Z., N.P., B.H., X.Z., C.Z. and K.G.P. made substantial revisions to all versions of the manuscript; all other named authors provided forest inventory data and commented on the manuscript.

Competing interests The authors declare no competing interests.

Additional information
Supplementary information is available for this paper at https://doi.org/10.1038/s41586-019-1128-0.
Reprints and permissions information is available at http://www.nature.com/reprints.
Correspondence and requests for materials should be addressed to T.W.C., J.L. or K.G.P.
Publisher's note: Springer Nature remains neutral with regard to jurisdictional claims in published maps and institutional affiliations.

GFBI consortium

Meinrad Abegg[16], C. Yves Adou Yao[17], Giorgio Alberti[18,19], Angelica Almeyda Zambrano[20], Esteban Alvarez-Davila[21], Patricia Alvarez-Loayza[22], Luciana F. Alves[23], Christian Ammer[24], Clara Antón-Fernández[25], Alejandro Araujo-Murakami[26], Luzmila Arroyo[26], Valerio Avitabile[27], Gerardo Aymard[28], Timothy Baker[29], Radomir Bałazy[30], Olaf Banki[31], Jorcely Barroso[32], Meredith Bastian[33], Jean-Francois Bastin[2], Luca Birigazzi[11], Philippe Birnbaum[162], Robert Bitariho[34], Pascal Boeckx[35], Frans Bongers, Olivier Bouriaud[36], Pedro H. S. Brancalion[37], Susanne Brandl[38], Francis Q. Brearley[39], Roel Brienen[29], Eben Broadbent[175], Helge Bruelheide[40,41], Filippo Bussotti[42], Roberto Cazzolla Gatti[43], Ricardo Cesar[37], Goran Cesljar[44], Robin Chazdon[45,46], Han Y. H. Chen[47,48], Chelsea Chisholm[49], Emil Cienciala[50,51], Connie J. Clark[52], David Clark[53], Gabriel Colletta[174], Richard Condit[55], David Coomes[56], Fernando Cornejo Valverde[57], Jose J. Corral-Rivas[58], Philip Crim[59,60], Jonathan Cumming[60], Selvadurai Dayanandan[61], André L. de Gasper[62], Mathieu Decuyper[8], Géraldine Derroire[63], Ben DeVries[64], Ilija Djordjevic[65], Amaral Ídeda[66], Aurélie Dourdain[63], Nestor Laurier Engone Obiang[67], Brian Enquist[68,69], Teresa Eyre[70], Adandé Belarmain Fandohan[71], Tom M. Fayle[72], Ted R. Feldpausch[73], Leena Finér[74], Markus Fischer[75], Christine Fletcher[76], Jonas Fridman[77], Lorenzo Frizzera[78], Javier G. P. Gamarra[11], Damiano Gianelle[78], Henry B. Glick[79], David Harris[80], Andrew Hector[81], Andreas Hemp[82], Geerten Hengeveld[8], John Herbohn[46], Martin Herold[8], Annika Hillers[83,178], Eurídice N. Honorio Coronado[84], Markus Huber[16], Cang Hui[85,86], Hyunkook Cho[87], Thomas Ibanez[88], Ilbin Jung[87], Nobuo Imai[89], Andrzej M. Jagodzinski[90,91], Bogdan Jaroszewicz[92], Vivian Johannsen[93], Carlos A. Joly[54], Tommaso Jucker[94], Viktor Karminov[95], Kuswata Kartawinata[22], Elizabeth Kearsley[96], David Kenfack[97], Deborah Kennard[98], Sebastian Kepfer-Rojas[93], Gunnar Keppel[99], Mohammed Latif Khan[100], Timothy Killeen[26], Hyun Seok Kim[101,102,103,104], Kanehiro Kitayama[105], Michael Köhl[106], Henn Korjus[107], Florian Kraxner[108], Diana Laarmann[107], Mait Lang[107], Simon Lewis[29,109], Huicui Lu[110], Natalia Lukina[111], Brian Maitner[68], Yadvinder Malhi[112], Eric Marcon[113], Beatriz Schwantes Marimon[114], Ben Hur Marimon-Junior[114], Andrew Robert Marshall[46,115,176], Emanuel Martin[116], Olga Martynenko[95], Jorge A. Meave[117], Omar Melo-Cruz[118], Casimiro Mendoza[119], Cory Merow[45], Abel Monteagudo Mendoza[120,121], Vanessa Moreno[37], Sharif A. Mukul[46,122], Philip Mundhenk[106], Maria G. Nava-Miranda[123], David Neill[124], Victor Neldner[70], Radovan Nevenic[65], Michael Ngugi[70], Pascal Niklaus[125], Jacek Oleksyn[90], Petr Ontikov[95], Edgar Ortiz-Malavasi[126], Yude Pan[127], Alain Paquette[128], Alexander Parada-Gutierrez[26], Elena Parfenova[129], Minjee Park[101], Marc Parren[130], Narayanaswamy Parthasarathy[131], Pablo L. Peri[132], Sebastian Pfautsch[133], Oliver Phillips[29], Maria Teresa Piedade[134], Daniel Piotto[135], Nigel C. A. Pitman[22], Irina Polo[136], Lourens Poorter[8], Axel Dalberg Poulsen[80], John R. Poulsen[52], Hans Pretzsch[137], Freddy Ramirez Arevalo[138], Zorayda Restrepo-Correa[139], Mirco Rodeghiero[78,177], Samir Rolim[135], Anand Roopsind[140], Francesco Rovero[141,142], Ervan Rutishauser[55], Purabi Saikia[143], Philippe Saner[125], Peter Schall[24], Mart-Jan Schelhaas[8], Dmitry Schepaschenko[108], Michael Scherer-Lorenzen[144], Bernhard Schmid[125], Jochen Schöngart[134], Eric Searle[47], Vladimír Seben[145], Josep M. Serra-Diaz[146,147], Christian Salas-Eljatib[179,180], Douglas Sheil[181], Anatoly Shvidenko[108], Javier Silva-Espejo[148], Marcos Silveira[149], James Singh[150], Plinio Sist[12], Ferry Slik[151], Bonaventure Sonké[152], Alexandre F. Souza[153], Krzysztof Stereńczak[30], Jens-Christian Svenning[147,154], Miroslav Svoboda[155], Natalia Targhetta[134], Nadja Tchebakova[129], Hans ter Steege[31,156], Raquel Thomas[157], Elena Tikhonova[111], Peter Umunay[79], Vladimir Usoltsev[158], Fernando Valladares[159], Fons van der Plas[160], Tran Van Do[161], Rodolfo Vasquez Martinez[120], Hans Verbeeck[96], Helder Viana[163,164], Simone Vieira[165], Klaus von Gadow[166], Hua-Feng Wang[167], James Watson[168], Bertil Westerlund[77], Susan Wiser[169], Florian Wittmann[170], Verginia Wortel[171], Roderick Zagt[172], Tomasz Zawila-Niedzwiecki[173], Zhi-Xin Zhu[167] & Irie Casimir Zo-Bi[13]

[16]Swiss Federal Institute for Forest, Snow and Landscape Research, WSL, Birmensdorf, Switzerland. [17]UFR Biosciences, University Félix Houphouët-Boigny, Abidjan, Côte d'Ivoire. [18]Department of Agricultural, Food, Environmental and Animal Sciences, University of Udine, Udine, Italy. [19]Institute of Biometeorology, National Research Council (CNR-IBIMET), Florence, Italy. [20]Spatial Ecology and Conservation Laboratory, Department of Tourism, Recreation and Sport Management, University of Florida, Gainesville, FL, USA. [21]Fundacion ConVida, Universidad Nacional Abierta y a Distancia, UNAD, Medellin, Colombia. [22]Field Museum of Natural History, Chicago, IL, USA. [23]Center for Tropical Research, Institute of the Environment and Sustainability, UCLA, Los Angeles, CA, USA. [24]Silviculture and Forest Ecology of the Temperate Zones, University of Göttingen, Göttingen, Germany. [25]Division of Forest and Forest Resources, Norwegian Institute of Bioeconomy Research (NIBIO), Ås, Norway. [26]Museo de Historia Natural Noel Kempff Mercado, Universidad Autonoma Gabriel Rene Moreno, Santa Cruz de la Sierra, Bolivia. [27]European Commission, Joint Research Centre, Ispra, Italy. [28]UNELLEZ-Guanare, Programa de Ciencias del Agro y el Mar, Herbario Universitario (PORT), Portuguesa, Venezuela. [29]School of Geography, University of Leeds, Leeds, UK. [30]Department of Geomatics, Forest Research Institute, Raszyn, Poland. [31]Naturalis Biodiversity Centre, Leiden, The Netherlands. [32]Centro Multidisciplinar, Universidade Federal do Acre, Rio Branco, Brazil. [33]Smithsonian's National Zoo and Conservation Biology Institute, Washington, DC, USA. [34]Institute of Tropical Forest Conservation, Mbarara University of Sciences and Technology, Mbarara, Uganda. [35]Isotope Bioscience Laboratory - ISOFYS, Ghent University, Ghent, Belgium. [36]Integrated Center for Research, Development and Innovation in Advanced Materials, Nanotechnologies, and Distributed Systems for Fabrication and Control (MANSiD), Stefan cel Mare University of Suceava, Suceava, Romania. [37]Department of Forest Sciences, Luiz de Queiroz College of Agriculture, University of São Paulo, Piracicaba, Brazil. [38]Bavarian State Institute of Forestry, Freising, Germany. [39]Manchester Metropolitan University, Manchester, UK. [40]Institute of Biology, Geobotany and Botanical Garden, Martin Luther University Halle-Wittenberg, Halle-Wittenberg, Germany. [41]German Centre for Integrative Biodiversity Research (iDiv) Halle-Jena-Leipzig, Leipzig, Germany. [42]Department of Agriculture, Food, Environment and Forest (DAGRI), University of Firenze, Florence, Italy. [43]Biological Institute, Tomsk State University, Tomsk, Russia. [44]Department of Spatial Regulation, GIS and Forest Policy, Institute of Forestry, Belgrade, Serbia. [45]Department of Ecology and Evolutionary Biology, University of Connecticut, Storrs, CT, USA. [46]Tropical Forests and People Research Centre, University of the Sunshine Coast, Maroochydore, Queensland, Australia. [47]Faculty of Natural Resources Management, Lakehead University, Thunder Bay, Ontario, Canada. [48]Key Laboratory for Humid Subtropical Eco-Geographical Processes of the Ministry of Education, Fujian Normal University, Fuzhou, China. [49]Institute of Integrative Biology, ETH Zürich, Zurich, Switzerland. [50]IFER - Institute of Forest Ecosystem Research, Jilove u Prahy, Czech Republic. [51]Global Change Research Institute CAS, Brno, Czech Republic. [52]Nicholas School of the Environment, Duke University, Durham, NC, USA. [53]Department of Biology, University of Missouri-St Louis, St Louis, MO, USA. [54]Department of Plant Biology, Institute of Biology, University of Campinas, UNICAMP, Campinas, Brazil. [55]Smithsonian Tropical Research Institute, Balboa, Panama. [56]Department of Plant Sciences, University of Cambridge, Cambridge, UK. [57]Andes to Amazon Biodiversity Program, Madre de Dios, Peru. [58]Facultad de Ciencias Forestales, Universidad Juárez del Estado de Durango, Durango, Mexico. [59]Department of Physical and Biological Sciences, The College of Saint Rose, Albany, NY, USA. [60]Department of Biology, West Virginia University, Morgantown, WV, USA. [61]Biology Department, Concordia University, Montreal, Quebec, Canada. [62]Natural Science Department, Universidade Regional de Blumenau, Blumenau, Brazil. [63]Cirad, UMR EcoFoG, Kourou, French Guiana. [64]Department of Geographical Sciences, University of Maryland, College Park, MD, USA. [65]Institute of Forestry, Belgrade, Serbia. [66]National Institute of Amazonian Research, Manaus, Brazil. [67]IRET, Herbier National du Gabon (CENAREST), Libreville, Gabon. [68]Department of Ecology and Evolutionary Biology, University of Arizona, Tucson, AZ, USA. [69]The Santa Fe Institute, Santa Fe, NM, USA. [70]Department of Environment and Science, Queensland Herbarium, Toowong, Queensland, Australia. [71]Ecole de Foresterie et Ingénierie du Bois, Université Nationale d'Agriculture, Ketou, Benin. [72]Biology Centre of the Czech Academy of Sciences, Institute of Entomology, Ceske Budejovice, Czech Republic. [73]Geography, College of Life and Environmental Sciences, University of Exeter, Exeter, UK. [74]Natural Resources Institute Finland (Luke), Joensuu, Finland. [75]Institute of Plant Sciences, University of Bern, Bern, Switzerland. [76]Forest Research Institute Malaysia, Kuala Lumpur, Malaysia. [77]Department of Forest Resource Management, Swedish University of Agricultural Sciences SLU, Umea, Sweden. [78]Department of Sustainable Agro-Ecosystems and Bioresources, Research and Innovation Center, Fondazione Edmund Mach, San Michele all'Adige, Italy. [79]School of Forestry and Environmental Studies, Yale University, New Haven, CT, USA. [80]Royal Botanic Garden Edinburgh, Edinburgh, UK. [81]Department of Plant Sciences, University of Oxford, Oxford, UK. [82]Department of Plant Systematics, University of Bayreuth, Bayreuth, Germany. [83]Centre for Conservation Science, The Royal Society for the Protection of Birds, Sandy, UK. [84]Instituto de Investigaciones de la Amazonía Peruana, Iquitos, Peru. [85]Centre for Invasion Biology, Department of Mathematical Sciences, Stellenbosch University, Stellenbosch, South Africa. [86]Theoretical Ecology Unit, African Institute for Mathematical Sciences, Cape Town, South Africa. [87]Division of Forest Resources Information, Korea Forest Promotion Institute, Seoul, South Korea. [88]Institut Agronomique néo-Calédonien (IAC), Equipe Sol & Végétation (SolVeg), Nouméa, New Caledonia. [89]Department of Forest Science, Tokyo University of Agriculture, Tokyo, Japan. [90]Institute of Dendrology, Polish Academy of Sciences, Kórnik, Poland. [91]Poznań University of Life Sciences, Department of Game Management and Forest Protection, Poznań, Poland. [92]Faculty of Biology, Białowieża Geobotanical Station, University of Warsaw, Białowieża, Poland. [93]Department of Geosciences and Natural Resource Management, University of Copenhagen, Copenhagen, Denmark. [94]Centre for Environment and Life Sciences, CSIRO Land and Water, Floreat, Western Australia, Australia. [95]Forestry Faculty, Bauman Moscow State Technical University, Mytischi, Russia. [96]CAVElab – Computational and Applied Vegetation Ecology, Department of Environment, Ghent University, Ghent, Belgium. [97]CTFS-ForestGEO, Smithsonian Tropical Research Institute, Balboa, Panama. [98]Department of Physical and Environmental Sciences, Colorado Mesa University, Grand Junction, CO, USA. [99]School of Natural and Built Environments and Future Industries Institute, University of South Australia, Adelaide, South Australia, Australia. [100]Department of Botany, Dr Harisingh Gour Central University, Sagar, India. [101]Department of Forest Sciences, Seoul National University, Seoul, South Korea. [102]Interdisciplinary Program in Agricultural and Forest Meteorology, Seoul National University, Seoul, South Korea. [103]National Center for Agro Meteorology, Seoul, South Korea. [104]Research Institute for Agriculture and Life Sciences, Seoul National University, Seoul, South Korea. [105]Graduate School of Agriculture, Kyoto University, Kyoto, Japan. [106]Institute for World Forestry, University of Hamburg, Hamburg, Germany. [107]Institute of Forestry and Rural Engineering, Estonian University of Life Sciences, Tartu, Estonia. [108]Ecosystems Services and Management, International Institute for Applied Systems Analysis, Laxenburg, Austria. [109]Department of Geography, University College London, London, UK. [110]Faculty of Forestry, Qingdao Agricultural University, Qingdao, China. [111]Center for Forest Ecology and Productivity, Russian Academy of Sciences, Moscow, Russia. [112]School of Geography, University of Oxford, Oxford, UK. [113]UMR EcoFoG, AgroParisTech, Kourou, France. [114]Departamento de Ciências Biológicas, Universidade do Estado de Mato Grosso, Nova Xavantina, Brazil. [115]Department of Environment & Geography, University of York, York, UK. [116]Department of Wildlife Management, College of African Wildlife Management, Mweka, Tanzania. [117]Departamento de Ecología y Recursos Naturales, Facultad de Ciencias, Universidad Nacional Autónoma de México, Mexico

City, Mexico. [118]Universidad del Tolima, Ibagué, Colombia. [119]Colegio de Profesionales Forestales de Cochabamba, Cochabamba, Bolivia. [120]Jardín Botánico de Missouri, Oxapampa, Peru. [121]Universidad Nacional de San Antonio Abad del Cusco, Cusco, Peru. [122]Department of Environmental Management, School of Environmental Science and Management, Independent University Bangladesh, Dhaka, Bangladesh. [123]Instituto de Silvicultura e Industria de la Madera, Universidad Juárez del Estado de Durango, Durango, Mexico. [124]Universidad Estatal Amazónica, Puyo, Pastaza, Ecuador. [125]Department of Evolutionary Biology and Environmental Studies, University of Zürich, Zürich, Switzerland. [126]Forestry School, Tecnológico de Costa Rica TEC, Cartago, Costa Rica. [127]Climate, Fire, and Carbon Cycle Sciences, USDA Forest Service, Durham, NC, USA. [128]Centre for Forest Research, Université du Québec à Montréal, Montréal, Quebec, Canada. [129]V. N. Sukachev Institute of Forest, FRC KSC, Siberian Branch of the Russian Academy of Sciences, Krasnoyarsk, Russia. [130]Department of Forestry, World Research Institute, Washington, DC, USA. [131]Department of Ecology and Environmental Sciences, Pondicherry University, Puducherry, India. [132]Instituto Nacional de Tecnología Agropecuaria (INTA), Universidad Nacional de la Patagonia Austral (UNPA), Consejo Nacional de Investigaciones Científicas y Tecnicas (CONICET), Rio Gallegos, Argentina. [133]School of Social Sciences and Psychology (Urban Studies), Western Sydney University, Penrith, New South Wales, Australia. [134]Instituto Nacional de Pesquisas da Amazônia, Manaus, Brazil. [135]Laboratório de Dendrologia e Silvicultura Tropical, Centro de Formação em Ciências Agroflorestais, Universidade Federal do Sul da Bahia, Itabuna, Brazil. [136]Jardín Botánico de Medellín, Medellín, Colombia. [137]Chair for Forest Growth and Yield Science, TUM School for Life Sciences, Technical University of Munich, Munich, Germany. [138]Universidad Nacional de la Amazonía Peruana, Iquitos, Peru. [139]Servicios Ecosistémicos y Cambio Climático (SECC), Fundación Con Vida & Corporación COL-TREE, Medellín, Colombia. [140]Department of Biological Sciences, Boise State University, Boise, ID, USA. [141]Tropical Biodiversity Section, MUSE - Museo delle Scienze, Trento, Italy. [142]Department of Biology, University of Florence, Florence, Italy. [143]Department of Environmental Sciences, Central University of Jharkhand, Ranchi, India. [144]Faculty of Biology, Geobotany, University of Freiburg, Freiburg im Breisgau, Germany. [145]National Forest Centre, Forest Research Institute Zvolen, Zvolen, Slovakia. [146]Université de Lorraine, AgroParisTech, Inra, Silva, Nancy, France. [147]Center for Biodiversity Dynamics in a Changing World (BIOCHANGE), Department of Bioscience, Aarhus University, Aarhus, Denmark. [148]Departamento de Biología, Universidad de la Serena, La Serena, Chile. [149]Centro de Ciências Biológicas e da Natureza, Universidade Federal do Acre, Rio Branco, Acre, Brazil. [150]Guyana Forestry Commission, Georgetown, French Guiana. [151]Faculty of Science, Universiti Brunei Darussalam, Bandar Seri Begawan, Brunei Darussalam. [152]Plant Systematic and Ecology Laboratory, Department of Biology, Higher Teachers' Training College, University of Yaoundé, Yaoundé, Cameroon. [153]Departamento de Ecologia, Universidade Federal do Rio Grande do Norte, Natal, Brazil. [154]Section for Ecoinformatics & Biodiversity, Department of Bioscience, Aarhus University, Aarhus, Denmark. [155]Faculty of Forestry and Wood Sciences, Czech University of Life Sciences, Prague, Czech Republic. [156]Systems Ecology, Free University Amsterdam, Amsterdam, The Netherlands. [157]Iwokrama International Centre for Rainforest Conservation and Development (IIC), Georgetown, French Guiana. [158]Botanical Garden of Ural Branch of Russian Academy of Sciences, Ural State Forest Engineering University, Ekaterinburg, Russia. [159]LINCGlobal, Museo Nacional de Ciencias Naturales, CSIC, Madrid, Spain. [160]Systematic Botany and Functional Biodiversity, Institute of Biology, Leipzig University, Leipzig, Germany. [161]Silviculture Research Institute, Vietnamese Academy of Forest Sciences, Hanoi, Vietnam. [162]Cirad, UMR-AMAP, CNRS, INRA, IRD, Université de Montpellier, Montpellier, France. [163]Centre for the Research and Technology of Agro-Environmental and Biological Sciences, CITAB, University of Trás-os-Montes and Alto Douro, UTAD, Vila Real, Portugal. [164]Agricultural High School, Polytechnic Institute of Viseu, Viseu, Portugal. [165]Environmental Studies and Research Center, University of Campinas, UNICAMP, Campinas, Brazil. [166]Department of Forest and Wood Science, University of Stellenbosch, Stellenbosch, South Africa. [167]Key Laboratory of Tropical Biological Resources, Ministry of Education, School of Life and Pharmaceutical Sciences, Hainan University, Haikou, China. [168]Division of Forestry and Natural Resources, West Virginia University, Morgantown, WV, USA. [169]Manaaki Whenua–Landcare Research, Lincoln, New Zealand. [170]Department of Wetland Ecology, Institute for Geography and Geoecology, Karlsruhe Institute for Technology, Karlsruhe, Germany. [171]Centre for Agricultural Research in Suriname (CELOS), Paramaribo, Suriname. [172]Tropenbios International, Wageningen, The Netherlands. [173]Polish State Forests, Coordination Center for Environmental Projects, Warsaw, Poland. [174]Programa de Pós-graduação em Biologia Vegetal, Instituto de Biologia, Universidade Estadual de Campinas, Campinas, Brazil. [175]Spatial Ecology and Conservation Laboratory, School of Forest Resources and Conservation, University of Florida, Gainesville, FL, USA. [176]Flamingo Land Ltd, Kirby Misperton, UK. [177]Centro Agricoltura, Alimenti, Ambiente, University of Trento, San Michele all'Adige, Italy. [178]Wild Chimpanzee Foundation, Liberia Office, Monrovia, Liberia. [179]Centro de Modelación y Monitoreo de Ecosistemas, Universidad Mayor, Santiago, Chile. [180]Laboratorio de Biometria, Universidad de La Frontera, Temuco, Chile. [181]Faculty of Environmental Sciences and Natural Resource Management, Norwegian University of Life Sciences, Ås, Norway.

METHODS

We quantified the relative abundance of tree symbiotic guilds across >1.1 million forest census plots combined in the GFBi database, an extension of the plot-based GFB database[31]. The GFBi database consists of individual-based data that we compiled from all the regional and national GFBi forest-inventory datasets. The standardized GFBi data frame (that is, tree list) comprises tree identifier (ID) (a unique number assigned to each individual tree); plot ID (a unique string assigned to each plot); plot coordinates, in decimal degrees of the WGS84 datum; tree size, in diameter-at-breast-height; trees-per-hectare expansion factor; year of measurement; dataset name (a unique name assigned to each forest inventory dataset); and binomial species names of trees.

We checked all species names from different forest inventory datasets for errors in three steps. First, we extracted scientific names from original datasets, and kept only the names of genus and species (authority names are removed). Next, we compiled all the species names into five general species lists (one for each continent). Finally, we verified individual species names against 23 online taxonomic databases using the 'taxize' package of the R programming language[32]. We assigned each morphospecies a unique name that comprised the genus, the string 'spp', followed by the dataset name and a unique number for that species. For example, 'Picea sppCNi1' and 'Picea sppCNi2' represent two different species under the genus *Picea*, observed in the first Chinese dataset (CNi).

We derived plot-level abundance information in terms of species-abundance matrices. Each species-abundance matrix consisted of the number of individuals by species (column vectors) within individual sample plots (row vectors). In addition, key plot-level information was also added to the matrices, including plot ID, dataset name, plot coordinates, the year of measurement and basal area (that is, the total cross-sectional areas (in m^2) of living trees per one hectare of ground area).

Tree genera were assigned to a plant family using a plant taxonomy lookup table generated by W. Cornwell (hosted on Github, https://github.com/traitecoevo/taxonlookup), which uses the accepted taxonomy from 'The Plant List' (http://www.theplantlist.org/). The majority (96.5%) of genera of the species in the GFBi were successfully matched to family; for those that could not be assigned, we manually checked the genus and species in the GFBi against synonyms from The Plant List. Of the 1,038 mismatches that remained after automated assignment to families, an additional 440 genera were assigned to family either by updating older genera and species names with their more-recent synonyms or by correcting obvious misspellings. The remaining 598 entries that could not be matched to family were excluded from further analysis.

We used a taxonomically informed approach to assign symbiotic states to plant species from the GFBi. Plant species were assigned to one of five symbiotic guilds; ectomycorrhizal, arbuscular mycorrhizal, ericoid mycorrhizal, weakly arbuscular mycorrhizal or non-mycorrhizal (AMNM) or N-fixer (Supplementary Table 1). Although we did not model the relative abundance of ericoid mycorrhizal trees (owing to their rarity), we have included a map of their relative abundance from our grid (Supplementary Fig. 1). We also include the full species list as Supplementary Data; this list includes the columns used to assign species to guilds. We also include a list of families and genera assigned to all guilds except the arbuscular mycorrhizal guild (Supplementary Tables 2–5), with notes for cases of species of individual genera that were assigned to two guilds simultaneously (for example, *Alnus* is an N-fixer and ectomycorrhizal) or for cases in which species from individual genera were split between two different guilds (for example, some *Pisonia* sp. are AMNM and some are ectomycorrhizal). An arbuscular mycorrhizal summary table is excluded from the Supplementary Tables for length considerations; this information is available as Supplementary Data (file name 'SymbioticGuildAssignment.csv').

The taxonomy of species in our inventory was compared with recently published literature on the evolutionary history of mycorrhizal symbiosis[7,33] and nitrogen fixation[34–37]. For most species, symbiotic status could be reliably assigned at the genus (for example, *Dicymbe*) or family level (for example, Pinaceae). For the few groups for which status was unreliable or variable within a genus (for example, *Pisonia*), we conducted additional literature searches.

We assigned species to the ectomycorrhizal category in three stages: first, at the family level (for example, Pinaceae); then, at the genus level (for example, *Dicymbe*); and, finally, by using literature searches for genera for which the status was unclear (for example, in the genus *Pisonia* some species are arbuscular mycorrhizal and others are ectomycorrhizal). We used a published list[38] to sort species into the appropriate guild. For the genus *Acacia*, we followed previous work[7] by assuming that only endemic Australian species associate with ectomycorrhizal fungi (we sorted *Acacia* species according to provenance using http://worldwidewattle.com/).

The AMNM category grouped all genera of terrestrial, non-epiphytic plants that either lack arbuscular mycorrhizal fungi or have low or inconsistent records of arbuscular mycorrhizal fungi colonization of roots. For example, although there are some published records of arbuscular mycorrhizal fungi colonization in the roots of plants of the Proteaceae family, these records are inconsistent and colonization is generally low. Further, as Proteaceae are associated with a non-mycorrhizal root morphology (the cluster or proteoid root system) that allows them to access otherwise unavailable forms of soil nutrients[39], we placed the entire family within AMNM. The family Urticaceae (which we also characterized as AMNM) was problematic—early successional species from tropical forests, such as those in the genus *Cecropia*, have records of both low and absent arbuscular mycorrhizal fungi colonization[40]. Our approach was to use the most broadly inclusive categorization for AMNM plants.

N-fixer status was assigned at the genus level, using previously compiled databases of global symbiotic N_2 fixation[34–37]. Given that symbiotic N_2 fixation with rhizobial or *Frankia* bacteria has evolved only in four orders (Rosales, Cucurbitales, Fabales and Fagales)[41], all species outside of this nitrogen-fixing clade were assigned non-fixing status. Some species could not be assigned an N-fixer status because they were typed to a higher taxonomic level (for example, family) that is ambiguous from the perspective of N-fixer status. We recorded when our assignment of N-fixer status was based on phylogenetic criteria, but where symbiotic nitrogen fixation is evolutionarily labile. Because these cases are more likely to be mis-assigned, we excluded them from the nitrogen-fixation category. The N-fixer group contains species that are colonized by arbuscular mycorrhizal fungi (for example, most genera from Leguminosae) and others that are colonized by ectomycorrhizal fungi (for example, *Alnus* sp.).

Most plant species form arbuscular mycorrhizal symbioses, the basal symbiotic state relative to the later-derived ectomycorrhizal and nitrogen-fixing symbioses. Furthermore, many ectomycorrhizal and nitrogen-fixing plants maintain the ability to form arbuscular mycorrhizal symbioses. Thus, a tree species is most likely to be arbuscular mycorrhizal if it does not form associations with another symbiotic guild (or forgoes root symbiosis entirely), as evidenced by its inclusion in exhaustive databases of plant symbiotic state[7,33–37,40]. In keeping with other large-scale studies in the field[33], we assigned tree species from the GFBi database an arbuscular-mycorrhizal-exclusive state if they belonged to taxa that were not matched to ectomycorrhizal, ericoid mycorrhizal, AMNM or N-fixer symbioses. Thus, the arbuscular mycorrhizal and N-fixer groups in our dataset are non-overlapping, despite the fact that most N-fixers also associate with arbuscular mycorrhizal fungi.

The proportions of tree basal area and tree individuals were aggregated to a 1°-by-1° grid by taking the weighted average of the plot-level proportions (Supplementary Table 6). This resulted in a total of 2,768 grid cells, each with a score for the proportional abundance of ectomycorrhizal, arbuscular mycorrhizal, N-fixer, ericoid mycorrhizal and AMNM trees. We calculated two measures of relative abundance for each symbiotic guild: the proportion of tree stems and the proportion of tree basal area. Because the measurements are highly correlated with one another (Supplementary Fig. 2), we chose to model only the proportion of total tree basal area, which should scale more closely to proportion of tree biomass as it accounts for differences in size among individual stems. Additionally, we quantified variability among plots within each grid cell by calculating the weighted standard deviation across the grid (Supplementary Information, Supplementary Figs. 3, 4).

To identify the key factors that structure symbiotic distributions, we assembled 70 global predictor layers: 19 climatic indices (relating to annual, monthly and quarterly temperature and precipitation variables), 14 soil chemical indices (relating to total soil nitrogen density, microbial nitrogen, C:N ratios and soil phosphorus fractions, pH and cation exchange capacity), 5 soil physical indices (relating to soil texture and bulk density), 26 vegetative indices (relating to leaf area index, total stem density, enhanced vegetation index means and variances) and 5 topographic variables (relating to elevation and hillshade) (Supplementary Table 7). Because decomposition is the dominant process by which soil nutrients become available to plants, we generated five additional layers that estimate climatic control of decomposition. We parameterized decomposition coefficients according to the Yasso07 model[20,42], using the following equation: $k = \exp(0.095T - 0.00014 \times T^2) \times (1 - \exp[-1.21 \times P])$, in which P and T are precipitation and mean temperature (either quarterly or annually) of a grid cell, and the constants 0.095, 0.00014 and −1.21 are parameters that were fit using a previous global study of leaf litter mass loss[20]. Although local decomposition rates can vary considerably based on litter quality or microbial community composition[43], climate is the primary control at the global scale[20]. Decomposition coefficients describe how fast different chemical pools of leaf litter lose mass over time, relative to a parameter (α) that accounts for leaf chemistry. Decomposition coefficients (k) with values of 0.5 and 2 indicate a halving and doubling of decomposition rates, respectively, relative to α (Supplementary Information, Supplementary Fig. 5).

We implemented the random-forest algorithm using the 'randomForest' package in R. Random-forest models average over multiple regression trees, each of which uses a random subset of all the model variables to predict a response. We first determined the influence and relationship of all 75 predictor layers on forest symbiotic state, and then optimized our models using a stepwise reduction in variables from least to most important. Variable importance was measured in two ways: increase in node purity and percentage increase in MSE (with values reported in Fig. 2). The increase in node purity of variable x considers the decrease in the residual sum of squares that results from splitting regression trees using variable x. The percentage increase in MSE quantifies the increase in model error as a result of randomly shuffling the order of values in the vector $\boldsymbol{x}$. We chose to rank variables according to the increase in node purity because we found that higher increases in node purities were associated with larger effect sizes, whereas larger percentage increases in MSE were associated with more-linear responses with smaller effect sizes. Whereas our inspection of partial feature contributions is derived from univariate random-forest models, we additionally ran multivariate random forests that predict the proportional abundance of ectomycorrhizal, arbuscular mycorrhizal and N-fixer trees for each pixel. The multivariate models were run using 50 regression trees each, with the unique set of the best 4 predictor variables for each symbiotic guild in the univariate models (Fig. 2, Supplementary Table 7). Despite strong negative correlations between the proportions of ectomycorrhizal and arbuscular mycorrhizal basal area (Supplementary Fig. 22), the results from multivariate and univariate random forests are strongly correlated with one another (Supplementary Fig. 23).

Using model selection based on eliminating variables with a low increase in node purity, we removed most soil nutrient, vegetative and topographic variables from our models (Supplementary Figs. 6, 7). Our final models include the remaining 34 predictor layers with climate, decomposition and some soil physical and chemical information (Supplementary Fig. 8). To determine the parsimony of our models, we compared the coefficient of determination in models run with a stepwise reduction in the number of variables (starting with those with the lowest increase in node purity). Based on performance of the ratio of coefficient of determination in models with 4 versus 34 variables, we determined that the 4 most-important variables accounted for >85% of the explained variability (Supplementary Fig. 9). We also compared model performance visually with plots of actual versus predicted proportions of each tree symbiotic guild among continents and geographical subregions (Supplementary Fig. 10). We used the 'forestFloor' package in R to plot the partial variable response of tree symbiotic guilds to each predictor variable (Fig. 2a–c, see Supplementary Figs. 19–21 for partial plots of the partial feature contributions of all 34 variables).

To test the sensitivity of model performance and predictions, we performed cross-validation in R using the 'rfUtilities' package[44]. K-fold cross-validation tests the sensitivity of model predictions to losing random subsets from the training data. For ectomycorrhizal, arbuscular mycorrhizal and N-fixer models, we ran 99 iterations that withheld 10% of the model training data. We assessed the decrease in model performance in the 99 iterations by manually calculating the coefficient of determination, which uses the following formula: $1 - \Sigma(\text{actual percentage basal area} - \text{predicted percentage basal area})^2/\Sigma(\text{actual percentage basal area} - \text{mean actual percentage basal area})^2$. For all symbiotic guilds, withholding 10% of the training data resulted in a mean loss in variance explained of less than 1% (Supplementary Fig. 11). This shows that our training data have sufficient redundancy to ensure that our model conclusions are robust. Similarly, to determine whether our random-forest models would make similar predictions if data were equally distributed among continents, we rarefied our aggregated grid of symbiotic states and predictor layers to an even depth. Specifically, we sub-sampled all continents—North America (including Central America and the Caribbean), South America, Europe, Asia and Oceania—to match the number of grid pixels from Africa ($n = 50$). This is a much more aggressive reduction of training data than is typically used in K-fold cross-validations, as it involves dropping ~90% of training data rather than retaining the same amount. We performed 99 iterations of rarefaction each for the three symbiotic guilds. On average, models run with the rarefied data explained about 10% less variance over the full training data (the entire predictor/response grid) than did models run with all of the training data (Supplementary Figs. 12, 13).

To avoid projecting our random-forest models outside the ranges of their training data (for example, grid cells with higher mean annual temperatures than the maximum used to fit the models), we subset a global grid of predictor layers depending on whether (1) the grid cell fell within the top 60% of land surface with respect to tree stem density[11] and either (2) fell within the univariate distribution of all the predictor layers from our training data and/or (3) fell within an 8-dimensional hypervolume defined by the unique set of the 4 best predictors of the relative abundance of each guild (Supplementary Fig. 14). We then projected our models across only those grid cells that met these criteria, which constitutes 46% of the global land surface and 88% of global tree stems (Fig. 1, Supplementary Fig. 15). Model projections were made at two resolutions: 1°-by-1° and 0.5°-by-0.5° (Fig. 4). Although model validation indicates that our projections are robust, additional studies to ground-truth these predictions and identify any discrepancies would be valuable. If such discrepancies exist, they can help to fine-tune climate–symbiosis models, or identify areas in which climate might favour invasion by symbioses that have not yet evolved in or dispersed to a particular biogeographical region.

We used the following equation to estimate the percentage of global tree stems that belong to each tree symbiotic guild: $\Sigma_i((\text{predicted proportion of trees of guild } g \text{ in pixel } i) \times (\text{total number of tree stems in pixel } i))/\Sigma_i(\text{total number of tree stems in pixel } i)$. The proportion of tree stems and the proportion of tree basal area in each guild are highly correlated throughout the training data (Supplementary Fig. 4). The figures cited in the main text for each guild were calculated using model projections across all pixels, even those that did not meet the criteria for model projection because they fell outside the multivariate distribution of the predictor layers or had insufficient stem density. However, our estimates for the global percentage of trees occupied by each tree symbiotic guild change by <1% when using only those pixels that met our criteria for model projection.

In the main text, we state that sharp transitions between dominant symbiotic states with climate variables could lead to declines in ectomycorrhizal trees, particularly in the southern range limit of the northern boreal forests. To determine this, we projected our random-forest models for each symbiotic guild using climate-change projections over our 19 bioclimatic variables (Supplementary Table 7), including the decomposition coefficients that use temperature and precipitation values. Specifically, we considered the 2070 scenario with a relative concentration pathway of 8.5 W per m^2, which predicts an increase of greenhouse gas emissions throughout the twenty-first century[45]. We plot the difference in the proportion of forest basal area between the projections for 2070 and projections that use current climate data (Supplementary Table 7, Supplementary Fig. 24). We qualify this prediction with the note that vegetative changes to forests are constrained by rates of mortality, recruitment and growth.

After training and cross-validating our models with GFBi data exclusively, we additionally tested whether our models accurately predicted the previously published[46] symbiotic state of Eurasian forests. We assigned symbiotic status to all of the trees in this previous publication, and aggregated plot-level data to a 1°-by-1° grid using the same methods as with the GFBi dataset (Supplementary Fig. 25). We found that—on average—our models predicted the symbiotic state in the regional dataset within 13.6% of the value of this previously published dataset (Supplementary Fig. 26). For projected maps in Fig. 4a–c, we included the previously published[46] data with the GFBi training data to increase geographical coverage throughout Eurasia.

Reporting summary. Further information on research design is available in the Nature Research Reporting Summary linked to this paper.

Data availability

Information regarding symbiotic guild assignments, model selection (including global rasters of our model projections for ectomycorrhizal, arbuscular mycorrhizal and N-fixer proportion of tree basal area) and analyses is available as Supplementary Data. The GFBi database is available upon written request at https://www.gfbinitiative.org/datarequest. Any other relevant data are available from the corresponding authors upon reasonable request.

31. Liang, J. et al. Positive biodiversity–productivity relationship predominant in global forests. *Science* **354**, aaf8957 (2016).
32. Chamberlain, S. A. & Szöcs, E. taxize: taxonomic search and retrieval in R. *F1000Res.* **2**, 191 (2013).
33. Brundrett, M. C. Mycorrhizal associations and other means of nutrition of vascular plants: understanding the global diversity of host plants by resolving conflicting information and developing reliable means of diagnosis. *Plant Soil* **320**, 37–77 (2009).
34. Werner, G. D., Cornwell, W. K., Sprent, J. I., Kattge, J. & Kiers, E. T. A single evolutionary innovation drives the deep evolution of symbiotic N_2-fixation in angiosperms. *Nat. Commun.* **5**, 4087 (2014).
35. Werner, G. D., Cornwell, W. K., Cornelissen, J. H. & Kiers, E. T. Evolutionary signals of symbiotic persistence in the legume–rhizobia mutualism. *Proc. Natl Acad. Sci. USA* **112**, 10262–10269 (2015).
36. Afkhami, M. E. et al. Symbioses with nitrogen-fixing bacteria: nodulation and phylogenetic data across legume genera. *Ecology* **99**, 502 (2018).
37. Tedersoo, L. et al. Global database of plants with root-symbiotic nitrogen fixation: Nod DB. *J. Veg. Sci.* **29**, 560–568 (2018).
38. Hayward, J. & Hynson, N. A. New evidence of ectomycorrhizal fungi in the Hawaiian Islands associated with the endemic host *Pisonia sandwicensis* (Nyctaginaceae). *Fungal Ecol.* **12**, 62–69 (2014).
39. Lambers, H., Martinoia, E. & Renton, M. Plant adaptations to severely phosphorus-impoverished soils. *Curr. Opin. Plant Biol.* **25**, 23–31 (2015).

40. Wang, B. & Qiu, Y.-L. Phylogenetic distribution and evolution of mycorrhizas in land plants. *Mycorrhiza* **16**, 299–363 (2006).
41. Soltis, D. E. et al. Chloroplast gene sequence data suggest a single origin of the predisposition for symbiotic nitrogen fixation in angiosperms. *Proc. Natl Acad. Sci. USA* **92**, 2647–2651 (1995).
42. Palosuo, T., Liski, J., Trofymow, J. & Titus, B. Litter decomposition affected by climate and litter quality—testing the Yasso model with litterbag data from the Canadian intersite decomposition experiment. *Ecol. Modell.* **189**, 183–198 (2005).
43. Bradford, M. A. et al. Climate fails to predict wood decomposition at regional scales. *Nat. Clim. Change* **4**, 625 (2014).
44. Evans, J. S. & Murphy, M. A. rfUtilities: random forests model selection and performance evaluation. R package version 2.1-3 https://cran.r-project.org/web/packages/rfUtilities/ (2018).
45. Core Writing Team et al. (eds) *Climate Change 2014 Synthesis Report* (IPCC, Geneva, 2014).
46. Schepaschenko, D. et al. A dataset of forest biomass structure for Eurasia. *Sci. Data* **4**, 170070 (2017).